

CO EMISSION FROM EVOLVED STARS AND PROTO-PLANETARY NEBULAE

G. R. KNAPP AND B. M. SUTIN
 Princeton University Observatory

AND

T. G. PHILLIPS, B. N. ELLISON, J. B. KEENE, R. B. LEIGHTON, C. R. MASSON,
 W. STEIGER, B. VEIDT, AND K. YOUNG
 California Institute of Technology

Received 1988 March 21; accepted 1988 June 23

ABSTRACT

We report the first observations of circumstellar CO emission from cool evolved giant stars using the Caltech 10.4 m submillimeter telescope. New detections, some tentative, were made of 16 stars, mostly south of -20° declination. Among the objects detected are the nearby S star π^1 Gru; the peculiar stars IRAS 15194–5115, IRAS 19500–1709, and IRAS 23321+6545; the supergiant OH/IR star VX Sgr; and possibly the WC10 Wolf-Rayet star CPD $-56^\circ 8032$ —this observation helps establish the identification of cool WC10 stars with planetary nebula nuclei. The CO outflow velocity for VX Sgr is $\sim 30 \text{ km s}^{-1}$, while that measured by OH maser emission is 19 km s^{-1} , showing that the wind velocity for VX Sgr continues to increase to very large distances from the star. The location of the peculiar cool stars on IRAS color-color diagrams and the detection of circumstellar CO suggests that they are proto-planetary nebulae.

Subject headings: nebulae: planetary — stars: circumstellar shells — stars: mass loss

I. INTRODUCTION

The stage of copious mass loss from cool evolved stars on the asymptotic giant branch is now accessible to study at infrared and millimeter wavelengths. Recent surveys in the CO rotational lines have resulted in the detection of CO(1–0) or CO(2–1) emission from more than 200 circumstellar envelopes (Knapp and Morris 1985; Zuckerman and Dyck 1986a, b; Zuckerman, Dyck, and Claussen 1986; Olofsson, Eriksson, and Gustafsson 1987; Rieu *et al.* 1988). These observations can be used to derive reasonably reliable values of the stellar velocity, of the terminal wind outflow velocity, and of the mass loss rate. The IRAS satellite (Neugebauer *et al.* 1984) has discovered several hundred thousand cool evolved stars, and eventually it is likely that detections of several hundred nearby evolved stars will be made in the thermal emission lines of CO. These data can be used to study such problems as the total rate of mass return to the interstellar medium by evolving stars, the chemical composition of the returned material, and the evolutionary state and progenitor masses of the stars. Further, the detection of molecular circumstellar shells around planetary nebulae (Mufson, Lyon and Marionni 1975) shows that the copious mass loss phase immediately precedes the formation of a planetary nebula.

Since the circumstellar molecular envelopes produced by mass loss from evolved stars are of small angular size, are centrally concentrated, and are warmer than typical molecular clouds, their emission is easier to detect in the higher- J CO transitions than in the CO(1–0) line, as shown by Knapp *et al.* (1982) and by Zuckerman and Dyck (1986a, b). The present paper discusses the first observations of circumstellar CO from evolved stars made with the 10.4 m telescope of the Caltech Submillimeter Observatory on Mauna Kea, Hawaii. Sixteen stars are newly detected. These observations take advantage of the high frequency and the superb site to make observations of greater sensitivity than has been available until fairly recently, and further exploit the observability of the southern sky

($\delta \geq -60^\circ$) from Hawaii—very little millimeter wavelength molecular line work has been done to date in the southern hemisphere. The observations are described in the next section, the objects are discussed individually and collectively in § III, and the conclusions are summarized in § IV.

II. OBSERVATIONS

a) Sample Selection

The objects to be observed were selected mostly from the IRAS Point Source Catalog (1985) to be (1) “hot” sources, i.e., the flux density falls with increasing wavelength; and (2) bright at $\lambda 12 \mu\text{m}$ and $\lambda 25 \mu\text{m}$. Since these observations were made during initial astronomical testing of the telescope, we observed stars with a wide range of properties (e.g., oxygen-rich and carbon-rich; small and large IR excesses; etc.). We concentrated on several objects of particular interest which had not been detected in previous observations (e.g., the supergiant OH/IR star VX Sgr) or which had not been observed due to their southerly declinations. Two classes of stars which have not previously received much attention at millimeter wavelengths are cool Wolf-Rayet (WC9 and later) stars with large infrared excesses, and the rare peculiar IRAS stars. We observed two WR stars, with a tentative detection of one of them, and four IRAS objects, with three detections. The positions of the observed sources, and their $12 \mu\text{m}$ and $25 \mu\text{m}$ flux densities, are listed in Table 1. The IRAS flux densities are as given in the Point Source Catalog and are not color corrected. Also given in Table 1 are the spectral types from the IRAS low-resolution spectrograph (IRAS Science Team 1986).

b) Observations

The observations were made in 1987 July at the CO(2–1) frequency of 230 GHz, using the Caltech 10.4 m telescope on Mauna Kea, Hawaii. The telescope beam efficiency and half-power beamwidth were, respectively, $\sim 67\%$ and $32''$ at the

TABLE 1
 OBSERVED STARS

Star	$\alpha(1950)$	$\delta(1950)$	$S_{12\mu\text{m}}$ (Jy)	$S_{25\mu\text{m}}$ (Jy)	LRS Class
IRAS 00193-4033	00 ^h 19 ^m 19 ^s .3	-40°33'51"	312	152	28
CRL 230	01 30 27.0	+62 11 25	289	455	37
R Hor	02 52 12.7	-50 05 32	729	311	24
CRL 4205	14 56 15.1	-54 06 16	93	310	80
CRL 4211	15 08 13.0	-48 08 44	793	423	42
IRAS 15194-5155	15 19 26.9	-51 15 19	1320	564	04
CRL 1822	16 02 59.7	-30 41 30	142	267	32
IRAS 16460-4022	16 46 05.9	-40 22 28	348	513	36
CPD -56°8032	17 04 47.5	-56 50 58	144	257	80
AH Sco	17 08 02.3	-32 15 53	629	349	28
OH 355.1-0.76	17 32 53.6	-33 27 50	767	562	29
VX Sgr	18 05 02.5	-22 13 56	2738	1385	26
IRAS 18276-1431	18 27 40.0	-14 31 05	23	132	05
IRAS 18467-4802	18 46 42.9	-48 02 42	285	343	22
S Sct	18 47 37.1	-07 57 59	65	17	...
IRC -30404	19 09 20.9	-32 56 06	319	210	28
CRL 2403	19 28 18.1	+19 44 19	88	179	39
AQ Sgr	19 31 27.0	-16 29 01	57	19	43
IRAS 19374+0550	19 37 26.2	+05 50 56	155	115	...
IRAS 19500-1709	19 50 01.5	-17 09 38	28	165	05
V1943 Sgr	20 03 51.7	-27 22 13	395	152	15
IRAS 20042-4241	20 04 15.7	-42 41 05	221	158	28
T Mic	20 24 51.9	-28 25 41	494	192	15
IRAS 21069-3843	21 06 57.1	-38 43 18	171	116	29
μ Cep	21 41 58.8	+58 32 58	1394	668	28
π^1 Gru	22 19 40.8	-46 12 06	908	436	42
β Gru	22 39 41.8	-47 08 49	942	238	...
V PsA	22 52 34.9	-29 52 46	247	110	22
IRAS 23321+6545	23 32 06.3	+65 45 15	14	86	05
R Aqr	23 41 14.0	-15 33 46	1577	543	...
PZ Cas	23 41 39.1	+61 30 43	373	398	69
IRC +60427	23 49 36.5	+61 31 33	369	255	27

zenith, but degraded at large zenith angles. The efficiency and beamwidth were measured by observations of Jupiter. The receiver used a liquid helium-cooled SIS junction (Ellison 1989) and was mounted at the Nasmyth focus. The observations were made in double-sideband mode with a receiver temperature of about 200 K. The antenna temperature scale and atmospheric opacity were measured for each source using a hot load. The antenna temperatures were corrected for beam efficiency and atmospheric extinction and are thus expressed as the Rayleigh-Jeans equivalent main beam brightness temperature seen by a perfect antenna of beamwidth $32''$ above the atmosphere. The telescope pointing and tracking, also monitored by observations of Jupiter, were better than $3''$ rms throughout the observations.

The spectral line backend was an acousto-optic spectrograph (Masson 1982) of 1024 channels, each of width 0.5 MHz ($=0.65 \text{ km s}^{-1}$ at 230 GHz). For each source, the observing frequency was set to correspond to 0 km s^{-1} with respect to the local standard of rest. The observations were made in position-switched mode; the position switching was usually $\pm 5'$ in azimuth except for stars near the Galactic plane, where $\pm 2'$ was used.

c) Data Reduction

Because of the relatively recent installation of the receiver on the telescope, intermittent baseline instability was a problem for this observing run. The individual on-off observations were examined, and those with bad baselines (about 15%) rejected. The remaining observations for each object were averaged and

corrected for atmospheric opacity and beam efficiency, and a linear or quadratic baseline was removed. Since the form of the baseline instability was a ripple of characteristic length about 200 km s^{-1} , it did not seriously affect the detectability of emission from circumstellar envelopes, for which the linewidths are usually $\leq 40 \text{ km s}^{-1}$. The integrated line intensity in units of $\text{K} \times \text{km s}^{-1}$, the peak line intensity, the central velocity V_c , and the half-width of the line at zero intensity (which is approximately the outflow velocity V_0) were found by inspection or by parabola fitting as described by Knapp and Morris (1985). The results are given in Table 2, where we list the source name, the galactic coordinates, the rms noise of the data, and, for the detected sources, the integrated line intensity $I_{\text{CO}} = \sum T_A^* dV$, the peak line intensity T_A^* , the central velocity V_c , and the outflow velocity V_0 . Quantities for the tentatively detected sources are enclosed in parentheses. Some of these observational results are uncertain because of contamination by narrow emission lines from Galactic plane CO clouds in the "on" or "off" beams: the stars so affected are IRAS 15194-5115, VX Sgr, and IRC +60427. In addition, there is contamination by Galactic CO emission over a wide velocity range for OH 355.1-0.7 and CRL 2403. It may be impossible to detect CO emission, should it exist, from these stars, and they will not be further discussed in this paper. CO emission was detected from 16 stars; the line profiles are shown in Figure 1.

Three previously known CO-line-emitting stars (*o* Cet, IRC +20326, and W Aql) were also observed as a check on the observing procedure; the results are in Table 3. The data are in satisfactory agreement with previous observations.

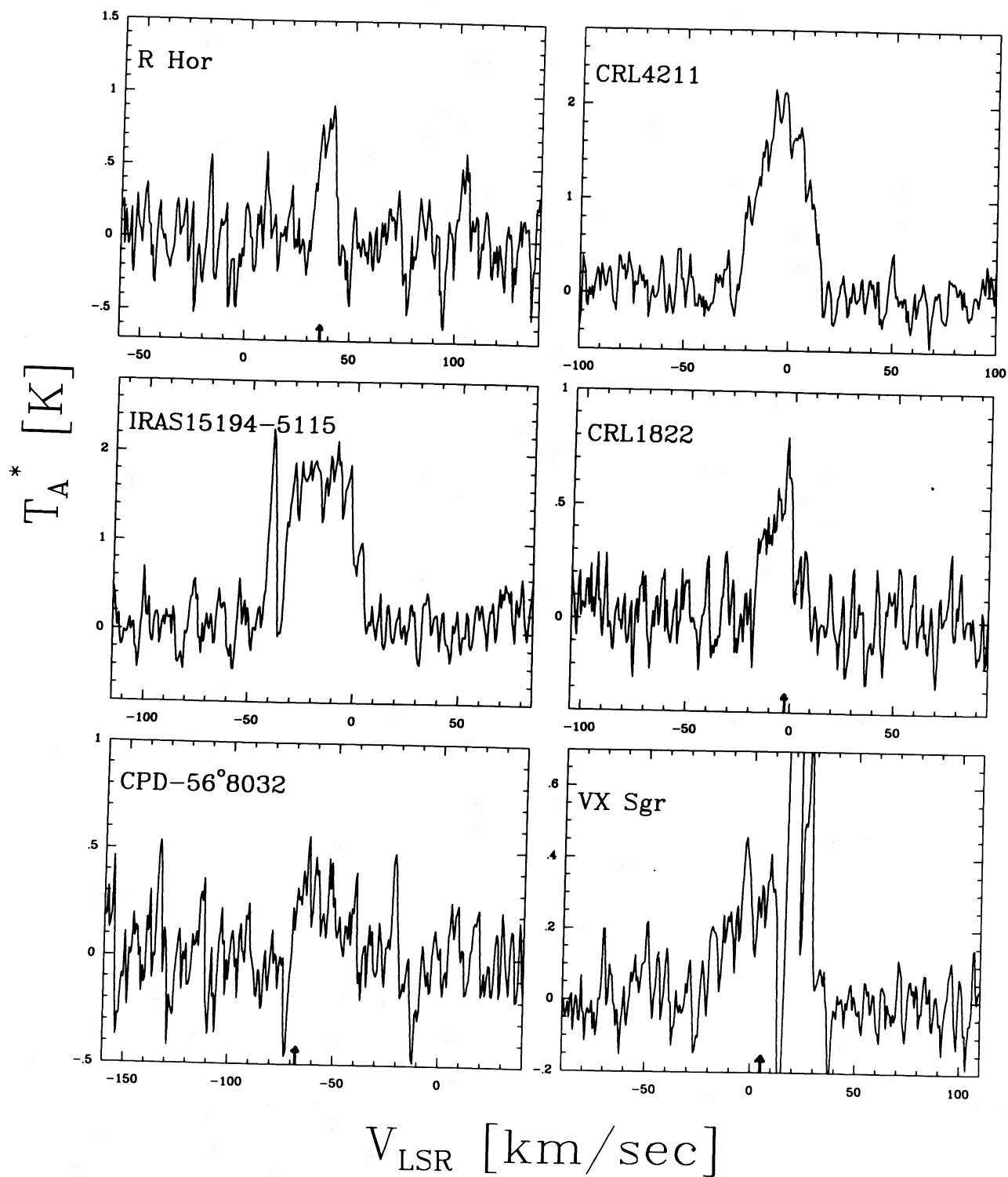


FIG. 1.—CO(2-1) line profiles for the 16 new stars detected in the present observations. The ordinate is Rayleigh-Jeans equivalent brightness temperature T_A^* in K; the abscissa velocity with respect to the local standard of rest. Radial velocities from other measurements are indicated by arrows on the velocity axis.

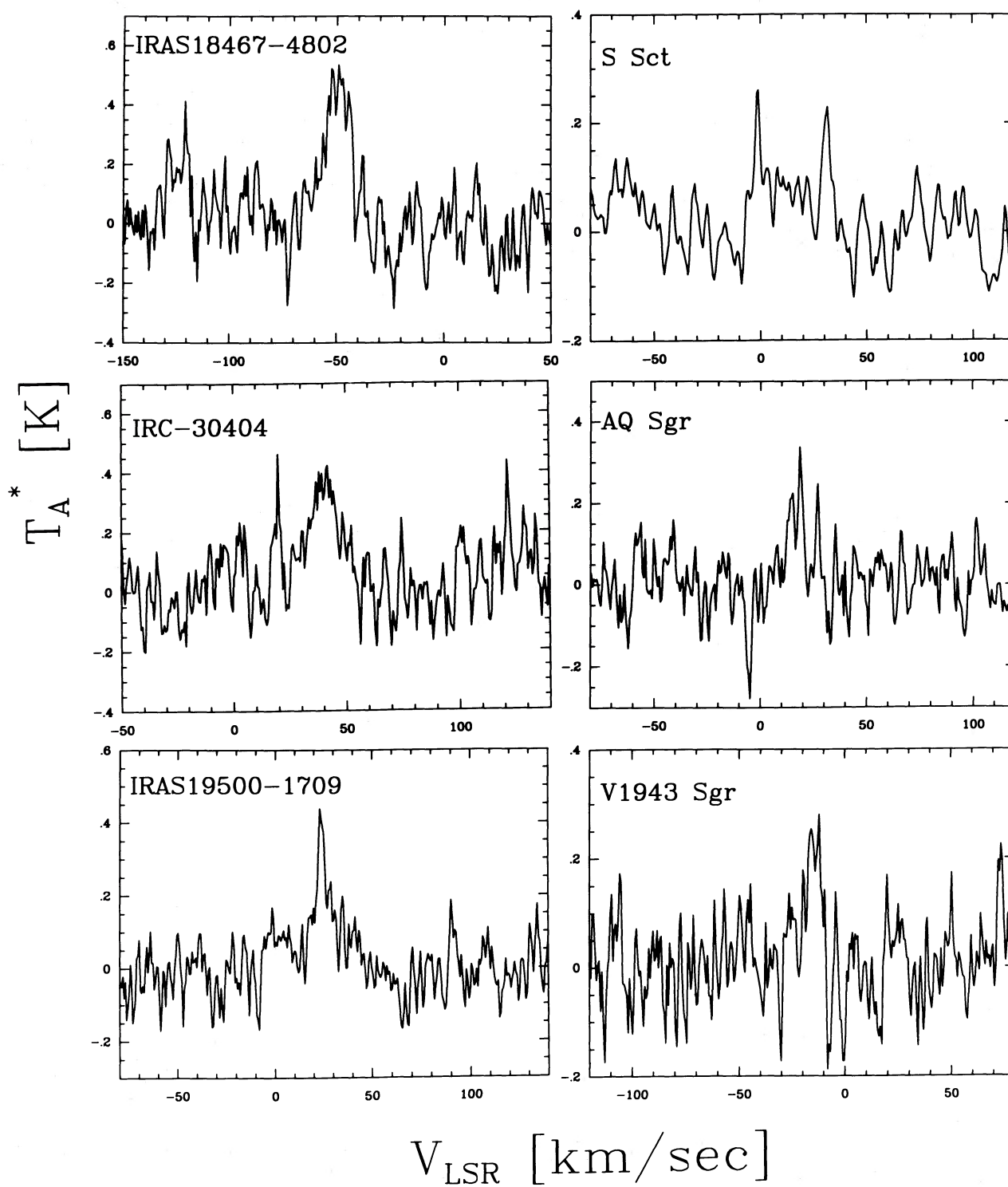


FIG. 1—Continued

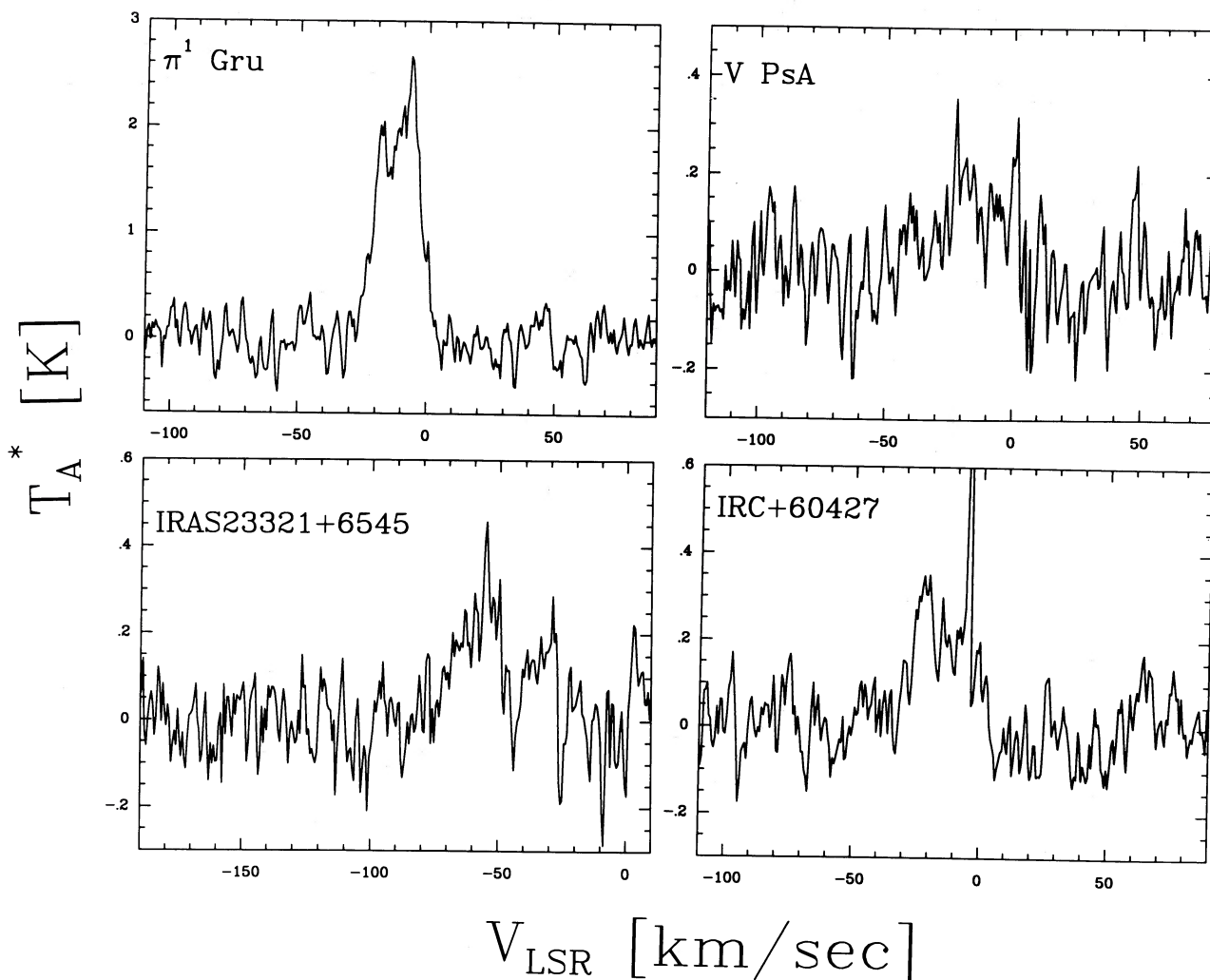


FIG. 1—Continued

III. RESULTS

a) Mass-Loss Rates

As discussed by Knapp *et al.* (1982) and Knapp and Morris (1985) observations of CO line emission can give reasonably reliable estimates for the mass-loss rates for evolved stars. Mass-loss rates were calculated for the 16 newly detected stars in this paper using modifications of the models described by Knapp and Morris (1985) and are listed in Table 4. The inputs to these models are as follows:

1. The wind outflow velocity V_0 , which is found from the CO observations.

2. The fractional abundance of CO: for carbon stars we assume $f = n(\text{CO})/n(\text{H}_2) = 8 \times 10^{-4}$, for S stars $f = 6 \times 10^{-4}$ and for stars with $n(\text{O}) > n(\text{C})$ (hereafter "oxygen" stars) $f = 3 \times 10^{-4}$. For many of the stars in our sample, the chemical type is known from optical spectroscopy (e.g., Lambert *et al.* 1986), from the presence of an OH maser, or from data from the IRAS low-resolution spectrometer (LRS) (IRAS Science Team 1986). There is no information available on the chemical composition of the peculiar IRAS sources; the mass loss rates were estimated using $f = 8 \times 10^{-4}$.

3. Distance: for the stars in the present sample, distance estimates have been made in a variety of ways, which will be described below when the individual stars are discussed. In many cases, we estimate the bolometric flux from the infrared data in the IRAS catalog and the compilation by Gezari, Schmitz, and Mead (1984) and find the distance assuming that the bolometric luminosity is $10^4 L_\odot$ (except for CPD -56°8032; see below), and ignoring interstellar extinction. For some stars, we have only the long-wavelength (IRAS) flux densities, and the resulting distances are uncertain by large factors. These estimates are enclosed in parentheses in Table 4.

4. For stars with low-mass loss rates the excitation of the CO rotational lines is primarily via excitation of the IR $v = 0 \rightarrow 1$ transition. The stellar luminosity density at $\lambda 4.7 \mu\text{m}$ was taken from the compilation by Gezari, Schmitz, and Mead (1984).

The mass-loss models have been changed slightly from those of Knapp and Morris (1985) by incorporating the results of recent CO photodissociation calculations by Mamon, Glassgold, and Huggins (1988). The outer radii of the CO shells in these models are smaller than those calculated from the models of Morris and Jura (1983).

TABLE 2
RESULTS

Star	l	b	rms (K)	I_{CO} (K \times km s $^{-1}$)	T_A^* (K)	V_c (km s $^{-1}$)	V_0 (km s $^{-1}$)
IRAS 00193–4033	326.04	–75.48	0.14
CRL 230 ^a	127.81	–0.02	0.14
R Hor	265.45	–57.38	0.21	5.4 \pm 0.8	0.8 \pm 0.2	+38.0 \pm 1.2	6.6 \pm 1.3
CRL 4205	321.05	+3.99	0.27
CRL 4211	325.55	+8.35	0.19	51.6 \pm 1.1	1.9 \pm 0.2	–3.7 \pm 0.8	20.5 \pm 1.5
IRAS 15194–5115 ^b	325.53	+4.66	0.23	58.5 \pm 1.5	1.9 \pm 0.2	–15.4 \pm 1.7	23.3 \pm 2.4
CRL 1822	344.99	+15.72	0.13	9.4 \pm 0.7	0.5 \pm 0.2	–5.3 \pm 1.8	14.2 \pm 3.8
IRAS 16460–4022	343.97	+2.72	0.26
CPD –56°8032	332.92	–9.91	0.17	(5.8 \pm 0.8)	0.3	–56	17)
AH Sco	353.08	+4.27	0.10
VX Sgr ^b	8.34	–1.00	0.07	11.2 \pm 0.5	~0.35	~ +6.5	~30
IRAS 18276–1431 ^a	17.68	–2.03	0.10
IRAS 18467–4802	348.22	–19.65	0.12	6.8 \pm 0.7	0.5 \pm 0.2	–50 \pm 4	11 \pm 2
S Sct	25.75	–3.35	0.06	(3.9 \pm 0.5)	0.11	+15	21)
IRC –30404	4.79	–18.44	0.10	7.3 \pm 0.5	0.3 \pm 0.1	+40 \pm 3	15 \pm 3
AQ Sgr	22.74	–16.70	0.07	(2.4 \pm 0.3)	0.25	+17	6)
IRAS 19374+0500	43.86	–7.95	0.06
IRAS 19500–1709	23.99	–21.04	0.07	(3.8 \pm 0.3)	0.3	+25	8)
V1943 Sgr	14.77	–27.68	0.07	(1.9 \pm 0.3)	0.2	–15	8)
IRAS 20042–4241	357.69	–31.50	0.17
T Mic	15.18	–32.43	0.15
IRAS 21069–3843	4.30	–42.85	0.11
μ Cep	100.60	+4.31	0.09
π^1 Gru	350.28	–55.16	0.08	42.2 \pm 1.0	2.1 \pm 0.2	–11.4 \pm 1.1	14.9 \pm 1.3
β Gru	346.27	–57.95	0.14
V PsA	20.48	–64.40	0.09	(3.7 \pm 0.4)	0.17	–15	21)
IRAS 23321+6545	115.21	+4.32	0.11	(7.5 \pm 0.6)	0.27	–59	15)
R Aqr	66.51	–70.33	0.06
PZ Cas	115.06	–0.05	0.13
IRC +60427 ^b	116.02	–0.27	0.07	6.3 \pm 0.5	0.25	–15	19

^a Narrow CO emission near 0 km s $^{-1}$.^b Galactic CO contaminating stellar emission.TABLE 3
RESULTS FOR PREVIOUSLY DETECTED CIRCUMSTELLAR ENVELOPES

Star	rms (K)	I_{CO} (K \times km s $^{-1}$)	T_A^* (K)	V_c (km s $^{-1}$)	V_0 (km s $^{-1}$)
α Cet	0.15	23.9 \pm 0.6	3.7 \pm 0.3	+45.8 \pm 0.3	5.0 \pm 0.4
W Aql	0.13	22.5 \pm 0.8	0.80 \pm 0.15	–25.3 \pm 2.9	21.1 \pm 2.0
IRC +20326	0.11	16.4 \pm 0.6	0.66 \pm 0.11	–5.2 \pm 3.0	18.4 \pm 3.5

TABLE 4
MASS-LOSS RATES

Star	Type, Period	Chemistry	Distance (pc)	\dot{M} (M_\odot yr $^{-1}$)
R Hor	M, 402 ^d	O	265	2.1 \times 10 $^{-7}$
CRL 4211	...	C	330	2.3 \times 10 $^{-6}$
IRAS 15194–5115	(400)	(6.1 \times 10 $^{-6}$)
CRL 1822	OH/IR	O	2000	2.9 \times 10 $^{-5}$
CPD –56°8032	WC10	C	(630)	(1.6 \times 10 $^{-6}$)
VX Sgr	M8I:SRV:732 ^d	O	1700	1.3 \times 10 $^{-5}$
IRAS 18467–4802	...	O	(870)	(3.8 \times 10 $^{-6}$)
S Sct	N3:C5, 4:SR:148 ^d	C	520	(6.9 \times 10 $^{-7}$)
IRC –30404	...	O	1400	1.1 \times 10 $^{-5}$
AQ Sgr	N3:C5:SRb:200 ^d	C	570	1.8 \times 10 $^{-7}$
IRAS 19500–1709 ^a	F8 or A + K	...	(1900)	(4.0 \times 10 $^{-6}$)
V1943 Sgr	M8	O	300	1.9 \times 10 $^{-7}$
π^1 Gru	S4, 7:LPV	S	200	1.3 \times 10 $^{-6}$
V PsA	M, SRb, 148 ^d	O	330	6.9 \times 10 $^{-7}$
IRAS 23321+6545	5000	(5.2 \times 10 $^{-5}$)
IRC +60427	M9	O	1000	5.8 \times 10 $^{-6}$

^a SAO 163075.

Table 4 gives the star name; the spectral and variable type and period, where known; the assumed chemistry; the assumed distance in pc; and the calculated mass loss rate in $M_{\odot} \text{ yr}^{-1}$.

b) Comparison with IRAS Data

The mass-loss rates derived for the stars in the present sample are compared with color data from the IRAS flux densities in Figures 2 and 3. Figure 2 shows a plot of mass-loss rate versus $S_{25 \mu\text{m}}/S_{12 \mu\text{m}}$ for the stars in the present sample and those from Knapp and Morris (1985); the mass-loss rate is roughly proportional to this ratio, and in general the evolved stars have $S_{12 \mu\text{m}} > S_{25 \mu\text{m}}$. However, the two peculiar red stars deviate markedly from this relationship, having much higher values of $S_{25 \mu\text{m}}/S_{12 \mu\text{m}}$ than stars with similar mass loss rates. Also plotted in Figure 2 are points corresponding to five planetary or proto-planetary nebulae (CRL 618, NGC 2346, VY 2-2, M1-92, and OH 231.8+4.2—all of these objects contain a hot component, as shown by the presence of radio continuum and/or optical line emission). The cool IRAS sources, and CPD -56°8032, occupy the same region of Figure 2 as do the planetary nebulae. In Figure 3, the ratio of the 60 μm to 25 μm flux densities is plotted versus the 25 μm to 12 μm ratio for the

same sample of stars and planetary nebulae. Van der Veen and Habing (1988) have discussed the evolution of AGB and post-AGB stars on this diagram. Again, the peculiar red IRAS stars occupy a similar part of the diagram to known planetary and proto-planetary nebulae.

c) Discussion

i) OH/IR Stars, Oxygen Stars, and VX Sgr

CO emission was detected from several OH/IR stars. R Hor is not detected at 1612 MHz but is weakly detected, with only one emission component, at 1665 and 1667 MHz (Robinson *et al.* 1971). The velocity of this component is $+36 \text{ km s}^{-1}$, in reasonable agreement with the CO velocity in Table 2. The distance of 225 pc is derived by Wilson *et al.* (1972) from the mid-infrared flux. The OH observations of CRL 1822 by Allen *et al.* give $V_c = -2.7 \text{ km s}^{-1}$ and $V_0 = 12.9 \text{ km s}^{-1}$, in good agreement with the CO values (Table 2).

Three other oxygen Mira stars, V1943 Sgr, IRC +60427, and V PsA, are also detected in the CO line. The IRAS LRS spectra for IRAS 18467-4802 and IRC -30404 show that these stars also have oxygen-rich circumstellar chemistry. The distances to all five of these stars were estimated by assuming that $L_{\text{bol}} = 10^4 L_{\odot}$.

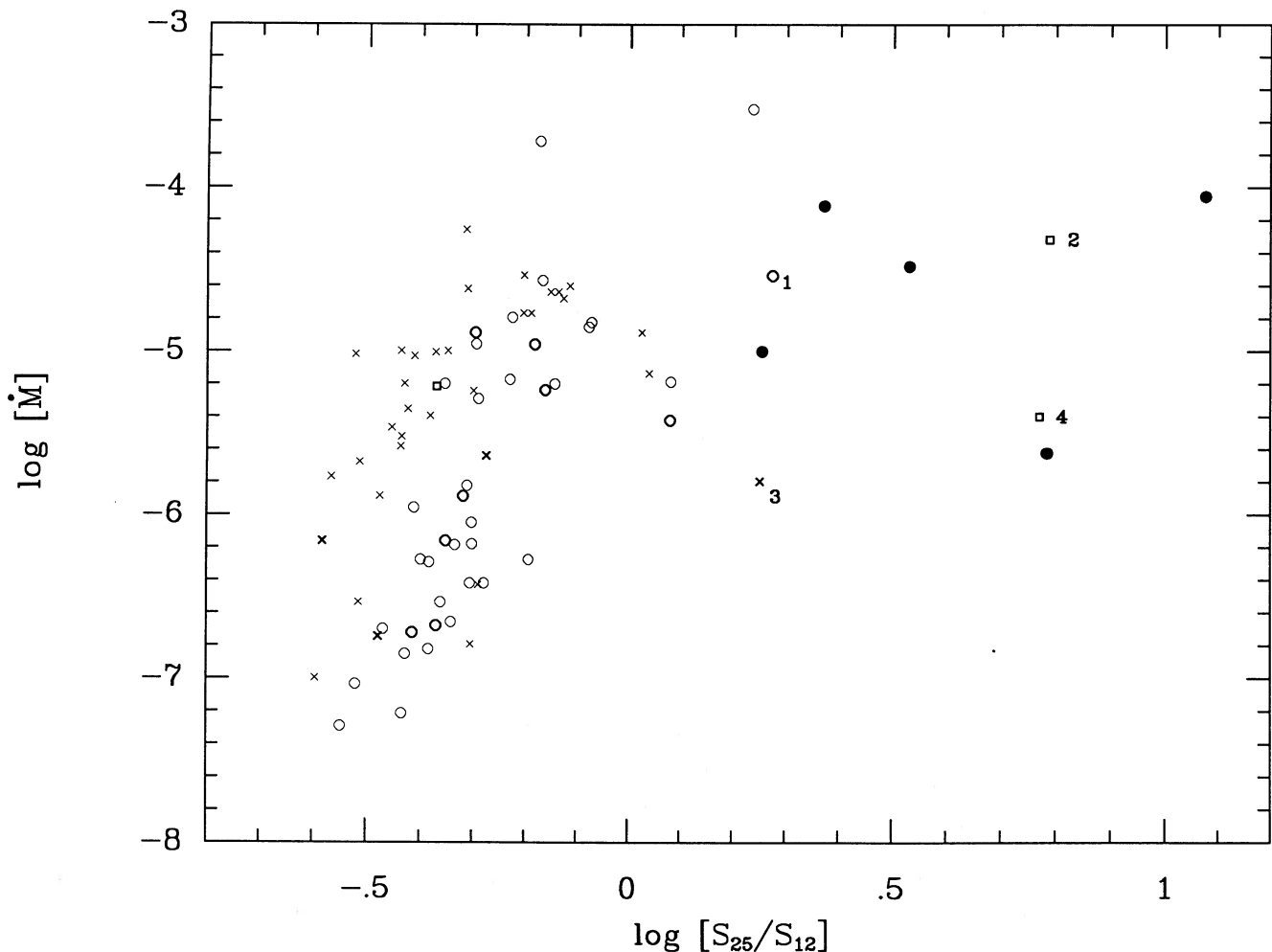


FIG. 2.—Mass loss rate \dot{M} vs. the ratio of IRAS 25 μm and 12 μm flux densities. (open circles): oxygen stars; (crosses): carbon and S stars; (open squares): peculiar IRAS stars. The stars from the present work are depicted by dark symbols, those from Knapp and Morris (1985) by light symbols; (filled circles): planetary and proto-planetary nebulae. The points are (1) CRL 1822, (2) IRAS 23321 + 6545, (3) CPD -56°8032, and (4) IRAS 19500-1709.

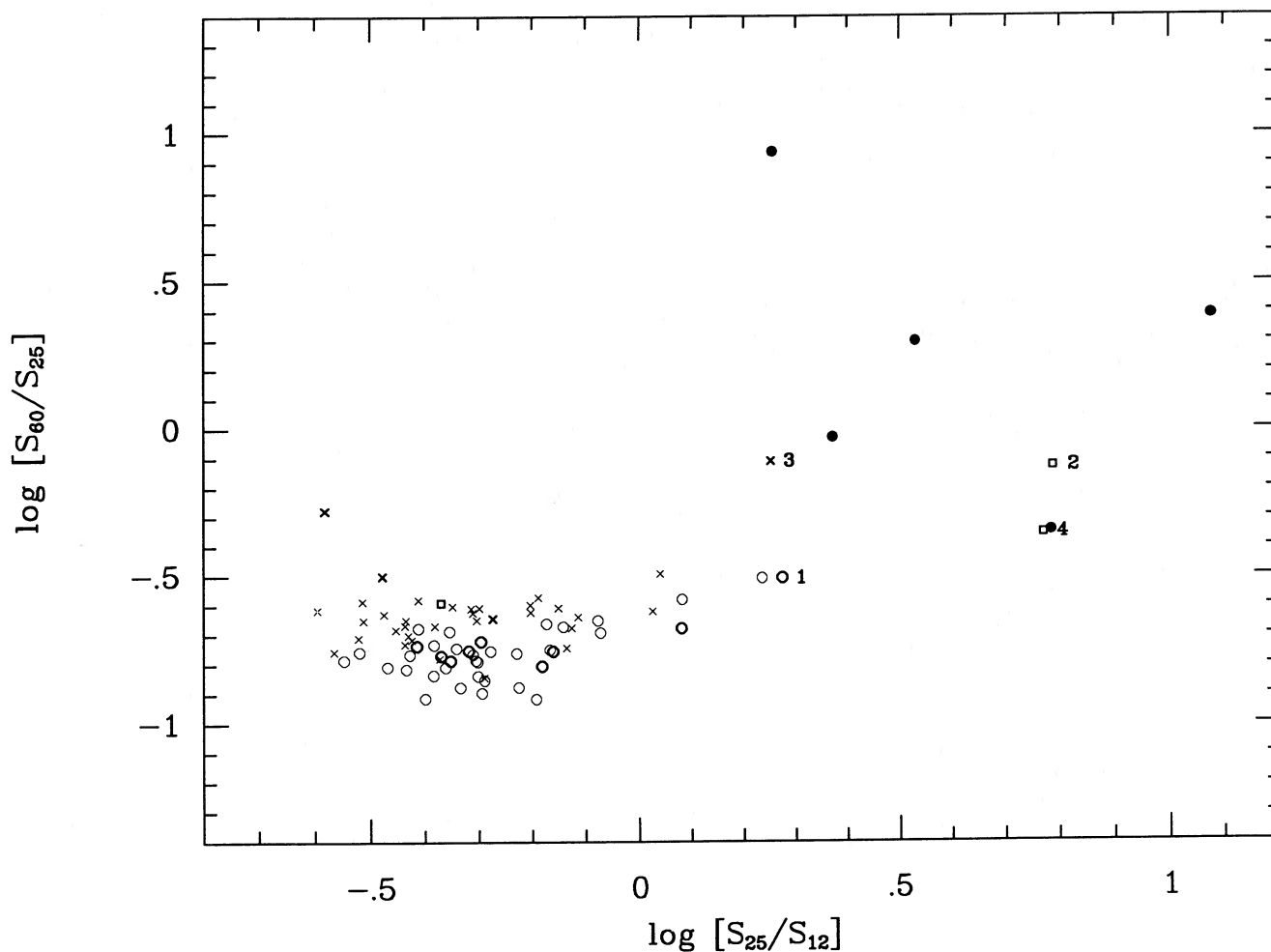


FIG. 3.—IRAS color-color plot for evolved stars and planetary nebulae detected in the CO line. The sample and symbols are the same as in Fig. 2.

By far the most interesting oxygen star detected is the OH/IR supergiant VX Sgr. This star has a luminosity of $4.6 \times 10^5 L_{\odot}$ (Humphreys, Strecker, and Ney 1972), and maps of its maser emission in the SiO, H₂O, OH 1665/7 MHz, and OH 1612 MHz lines show that the wind outflow velocity continues to rise smoothly to very large distances from the star ($> 85R_{*}$, or 2×10^{16} cm, the radius of the 1612 MHz OH maser) (Chapman and Cohen 1986). This behavior is contrary to that predicted by models where the spherically symmetric wind is accelerated to its terminal velocity by radiation pressure, in which all of the acceleration takes place within a few stellar radii. The velocity of the OH 1612 MHz maser is 19 km s^{-1} ; Chapman and Cohen (1986) suggest that the acceleration is caused by continued grain growth and predict a terminal wind velocity of 28 km s^{-1} .

The CO emission, which comes from the whole envelope but is heavily weighted by emission at large radii, has a terminal velocity of $\sim 30 \text{ km s}^{-1}$. This value is probably not much affected by the contamination by Galactic plane CO emission seen in the line profile (Fig. 1), since the CO central velocity ($+6.5 \text{ km s}^{-1}$) agrees well with that given by the masers ($+5.3 \text{ km s}^{-1}$). The outer radius of the CO shell is probably determined by photodissociation, and the models of Mamon, Glassgold, and Huggins (1988) give a photodissociation radius of $\sim 2 \times 10^{17}$ cm, about 20 times the 1612 MHz OH maser

radius. The CO observation thus confirms that the wind velocity continues to rise to very large distances from the star; the CO velocity is in good agreement with the terminal velocity predicted by Chapman and Cohen (1986).

The distance estimate for VX Sgr in Table 2 comes from its possible membership of the Sgr OB1 association (Humphreys, Strecker, and Ney 1972). The mass-loss rate found from the CO emission ($1.5 \times 10^{-5} M_{\odot} \text{ yr}^{-1}$; Table 3) agrees reasonably well with estimates from the OH maser shell radius ($2.5 \times 10^{-5} M_{\odot} \text{ yr}^{-1}$; Netzer 1989), from models of the mid-infrared dust emission ($2.1 \times 10^{-5} M_{\odot} \text{ yr}^{-1}$; Rowan-Robinson and Harris 1983) and from the $[2.2 \mu\text{m}] - [25 \mu\text{m}]$ color ($1.3 \times 10^{-5} M_{\odot} \text{ yr}^{-1}$; Knapp and Wilcots 1986). These mass-loss rate estimates use radiation from different parts of the envelope. The infrared estimates, based on emission from the dust, give the mass-loss rate at a few stellar radii from the star. The OH maser shell is at a distance of about 2×10^{16} cm from the star, while the CO emission is heavily weighted by emission at yet larger distances, up to about 2×10^{17} cm. The observed velocity gradient in the envelope therefore cannot be accounted for by a change in the mass-loss rate. Neither can it be due to continued acceleration of the wind due to grain growth, as shown by Netzer (1989).

If the gradient were due to a luminosity decrease of the star, VX Sgr would have decreased its luminosity by about a factor

of 10 during the last 2000 yr (the crossing time of the CO envelope) from a value of $5 \times 10^6 L_{\odot}$. Perhaps a more plausible explanation is that the density distribution is not spherically symmetric, but has an equatorial density enhancement (a thick disk) which is highly inclined to the line of sight, and where the maser emission is produced. This geometry is similar to that proposed to several other OH/IR stars, for example OH 231.8 + 4.2 (Bowers and Morris 1984).

ii) Carbon and S Stars

CO emission was detected from three carbon stars (CRL 4211, S Sct, and AQ Sgr), and from the S star π^1 Gru. S Sct and AQ Sgr are bright carbon stars from the study by Lambert *et al.* (1986). The distances to both of these stars were estimated using the K magnitudes given by Lambert *et al.* (1986) and assuming $M_K = -8$ mag. The detection of CO emission from S Sct is extremely tentative. A recent CO(1–0) observation at the IRAM 30 m telescope (Jura 1987) also finds emission at a radial velocity of $+15.8 \text{ km s}^{-1}$, so the presence of CO emission is confirmed.

π^1 Gru is the only S star in the sample. Its distance is estimated at 200 pc using the brightness of its G0 V companion (Feast 1953) and its possible association with the Hyades moving group (Eggen 1972). The latter identification is of interest because the age of the Hyades (10^9 yr) suggests that the progenitor mass of π^1 Gru is $\sim 2.5 M_{\odot}$.

iii) Wolf-Rayet Stars

Two late-type Wolf-Rayet stars with large infrared excesses (cf. Webster and Glass 1974; Cohen and Barlow 1980; Aitken *et al.* 1980), CRL 4205 and CPD $-56^{\circ}8032$, were observed in the CO line, and the latter was tentatively detected (Fig. 1). This object is classified as a cool carbon Wolf-Rayet star (WC10 or WC11). WC10 stars are defined as having lower excitation than normal W-R stars by Webster and Glass (1974), who suggest that these stars are related to the WC Population II stars which occur as planetary nebula nuclei. The presence of the CO emission establishes this connection—CPD $-56^{\circ}8032$ joins the small class of planetary nebulae in which the molecular circumstellar shell produced by the previous AGB mass-loss phase is not yet completely ionized by the central hot star—NGC 7027 is a Population I analog. Since CPD $-56^{\circ}8032$ is a carbon W-R star, we assume that the surrounding circumstellar material has carbon-star composition.

Cowley and Hiltner (1969) show that the stellar emission lines are narrow and of low excitation, and conclude that CPD $-56^{\circ}8032$ is not a conventional W-R star, in agreement with the above conclusions. They measure an emission-line radial velocity (with respect to the LSR) of -69 km s^{-1} , which is in reasonable agreement with the CO value (Table 2). Since the object is 10° out of the Galactic plane, it is unlikely that there is much contribution from Galactic rotation—rather, this high velocity is consistent with the identification of CPD $-56^{\circ}8032$ as a Population II object. The distance to this object is unknown. Since the exciting stars of planetary nebulae are expected (Paczynski 1971) and observed (Knapp *et al.* 1982; Jura 1984; Knapp 1986) to decrease rapidly in luminosity at the end of the mass-losing phase and at the onset of planetary nebula formation, we have assumed an intrinsic luminosity of $10^3 L_{\odot}$ in estimating the distance.

This detection, if confirmed, is the first of circumstellar CO emission from a Wolf-Rayet star. Since the lifetimes of the

circumstellar envelopes are very short ($\leq a \text{ few} \times 10^3$ yr; Spergel, Giuliani, and Knapp 1983) once photoionization has begun, this detection not only connects the late WC stars with planetary nebula nuclei but also suggests that they may be very recently formed.

iv) Peculiar IRAS Sources

The IRAS LRS atlas contains spectra of a small number of objects with peculiar cool spectra, classified 0_n (these classifications are given in Table 1). Likkell *et al.* (1987) and van der Veen and Habing (1988) suggest that the peculiar red objects are stars evolving toward planetary nebulae. We observed four of these stars and detected CO emission from three of them (IRAS 15194–5115 [blue], IRAS 19500–1709 [red], and IRAS 23321+6545 [red]). The distance and mass-loss rate estimates for these objects are extremely uncertain and are enclosed in parentheses in Table 4. CO(1–0) emission has been detected from IRAS 19500–1709 and IRAS 23321+6545 by Likkell *et al.* (1987) using the IRAM 30 m telescope—the measurements for both stars are in very good agreement. IRAS 19500–1709 is identified with the 9th mag star SAO 163075, whose spectral type is F8 (SAO) or A+K (N. Sanduleak, quoted by Likkell *et al.* 1987).

The distance to IRAS 23321+6545 is probably somewhat better determined than for the other two stars—it is in the Galactic plane and has a fairly high radial velocity. The kinematic distance is 6 kpc, in reasonably agreement with the value of 5 kpc obtained from the bolometric luminosity of $10^4 L_{\odot}$. These three IRAS sources have mass-loss rates in the range of values found for AGB stars. The blue object, IRAS 15194–5115, has similar infrared colors, but the two detected red stars have considerably redder colors (Figs. 2 and 3), and occupy the same regions of these infrared color-color diagrams as do known planetary and protoplanetary nebulae. They are thus very strong proto-planetary nebula candidates.

IV. CONCLUSIONS

This paper describes a search for CO(2–1) line emission from 30 evolved stars with a wide range of properties. Emission was detected from both carbon and oxygen stars, and from one S star, π^1 Gru.

The CO outflow velocity for the OH/IR supergiant star VX Sgr is about 30 km s^{-1} , considerably higher than that given by the OH maser emission, 19 km s^{-1} . The wind velocity appears to continue to increase to very large distances, perhaps greater than 10^{17} cm, from the star.

Two cool Wolf-Rayet stars were observed, and one, CPD $-56^{\circ}8032$, was tentatively detected. This observation confirms the identification of cool W-R stars with planetary nebula nuclei, and suggests that these nuclei are recently formed.

Circumstellar CO emission was also detected from three of the peculiar IRAS stars. Two of them are peculiar red objects, have mass-loss rates in the range of those observed for AGB stars, and occupy the same region of IRAS color-color plots as do planetary and proto-planetary nebulae. They are thus strong candidates for evolved stars in transition to the planetary nebula phase.

The Caltech Submillimeter Observatory is supported by the National Science Foundation under grant AST 83-11849. The SIS junctions were made at AT & T Bell Laboratories by R. E. Miller. This research is also supported by N.S.F. grant AST87-62945 to Princeton University.

REFERENCES

- Aitken, D. A., Barlow, M. J., Roche, P. F., and Spenser, P. M. 1980, *M.N.R.A.S.*, **192**, 679.
- Allen, D. A., Hyland, A. R., Longmore, A. J., Caswell, J. L., Goss, W. M., and Haynes, R. F. 1977, *Ap. J.*, **217**, 108.
- Bowers, P. F., and Morris, M. 1984, *Ap. J.*, **276**, 646.
- Chapman, J. M., and Cohen, R. J. 1986, *M.N.R.A.S.*, **220**, 513.
- Cohen, M., and Barlow, M. J. 1980, *Ap. J.*, **238**, 585.
- Cowley, A. P., and Hiltner, W. A. 1969, *Astr. Ap.*, **3**, 513.
- Eggen, O. J. 1972, *Ap. J.*, **177**, 489.
- Ellison, B. N. 1989, in preparation.
- Feast, M. W. 1953, *M.N.R.A.S.*, **174**, 711.
- Gezari, D. Y., Schmitz, M., and Mead, J. M. 1984, *Catalog of Infrared Observations* (NASA Ref. Pub. 1118).
- IRAS Point Source Catalog*. 1985, Joint IRAS Science Working Group (Washington, D.C.: U.S. Government Printing Office).
- IRAS Science Team. 1986, *Astr. Ap. Suppl.*, **65**, 607.
- Humphreys, R. M., Strecker, D. W., and Ney, E. P. 1972, *Ap. J.*, **172**, 75.
- Jura, M. 1984, *Ap. J.*, **282**, 200.
- . 1987, private communication.
- Knapp, G. R. 1986, *Mitt. Astr. Ges.*, **67**, 111.
- Knapp, G. R., and Morris, M. 1985, *Ap. J.*, **292**, 640.
- Knapp, G. R., Phillips, T. G., Leighton, R. B., Lo, K.-Y., Wannier, P. G., Wootten, H. A., and Huggins, P. J. 1982, *Ap. J.*, **252**, 616.
- Knapp, G. R., and Wilcots, E. P. 1986, in *Late Stages of Stellar Evolution*, ed. S. Kwok and S. R. Pottasch (Dordrecht: Reidel), p. 171.
- Lambert, D. L., Gustafsson, B., Eriksson, K., and Hinkle, K. H. 1986, *Ap. J. Suppl.*, **62**, 373.
- Likkel, L., Omont, A., Morris, M., and Forveille, T. 1987, *Astr. Ap.*, **173**, L11.
- Mamon, G. A., Glassgold, A. E., and Huggins, P. J. 1988, *Ap. J.*, **328**, 397.
- Masson, C. R. 1982, *Astr. Ap.*, **114**, 270.
- Morris, M., and Jura, M. 1983, *Ap. J.*, **264**, 546.
- Mufson, S. L., Lyon, J., and Marionni, P. A. 1975, *Ap. J. (Letters)*, **201**, L85.
- Netzer, N. 1989, in preparation.
- Neugebauer, G., et al. 1984, *Ap. J. (Letters)*, **278**, L1.
- Olofsson, H., Eriksson, K., and Gustafsson, B. 1987, *Astr. Ap.*, **183**, L13.
- Pacyński, B. 1971, *Acta Astr.*, **21**, 271.
- Rieu, N. G., Epchtein, N., Bach, T., and Cohen, M. 1988, *Astr. Ap.*, in press.
- Robinson, B. J., et al. 1971, *Ap. Letters*, **7**, 163.
- Rowan-Robinson, M., and Harris, S. 1983, *M.N.R.A.S.*, **202**, 767.
- Spergel, D. N., Giuliani, J. L., and Knapp, G. R. 1983, *Ap. J.*, **275**, 330.
- van der Veen, W. E. C. J., and Habing, H. J. 1988, *Astr. Ap.*, **194**, 125.
- Webster, B. L., and Glass, I. S. 1974, *M.N.R.A.S.*, **166**, 491.
- Wilson, W. J., Schwartz, P. R., Neugebauer, G., and Becklin, E. E. 1972, *Ap. J.*, **177**, 523.
- Zuckerman, B., and Dyck, H. M. 1986a, *Ap. J.*, **304**, 394.
- . 1986b, *Ap. J.*, **311**, 345.
- Zuckerman, B., Dyck, H. M., and Claussen, M. J. 1986, *Ap. J.*, **304**, 401.

B. N. ELLISON, J. B. KEENE, R. B. LEIGHTON, C. R. MASSON, T. G. PHILLIPS, B. VEIDT, and K. YOUNG: 320-47, California Institute of Technology, Pasadena, CA 91125

G. R. KNAPP: Princeton University Observatory, Princeton, NJ 08544

W. STEIGER: Caltech Submillimeter Observatory, P.O. Box 4339, Hilo, HI 96720

B. M. SUTIN: Astronomy Program, University of Maryland, College Park, MD 20742